Anomalous magnetic properties and non-Fermi-liquid behaviour in single crystals of the Kondo lattice $CeNiGe_{2-x}Si_x$

2004 J. Phys.: Condens. Matter 16 8323

(http://iopscience.iop.org/0953-8984/16/46/018)

INSTITUTE OF PHYSICS PUBLISHING JOURNAL OF PHYSICS: CONDENSED MATTER

J. Phys.: Condens. Matter **16** (2004) 8323–8334 PII: S0953-8984(04)85233-0

Anomalous magnetic properties and non-Fermi-liquid behaviour in single crystals of the Kondo lattice $CeNiGe_{2-x}Si_x$

D Y Kim[1,2], D H Ryu[1,2], J B Hong[1,2], J-G Park[1,2], Y S Kwon[1,2,7], M A Jung[3], M H Jung[4], N Takeda[5], M Ishikawa[5] and S Kimura[6]

[1] BK21 Physics Research Division and Institute of Basic Science, Sungkyunkwan University, Suwon 440-746, Korea
[2] Centre for Strongly Correlated Material Research, Seoul National University, Seoul 151-742, Korea
[3] Interdisciplinary Programme in Nanoscience and Technology, Sungkyunkwan University, Suwon 440-746, Korea
[4] National Research Laboratory for Material Science, Korea Basic Science Institute, 52 Yeoeun-Dong Yusung-Gu, Daejeon 305-333, Korea
[5] Institute for Solid State Physics, University of Tokyo, Kashiwanoha, Kashiwa, Chiba 277-8581, Japan
[6] UVSOR Facility, Institute for Molecular Science, Okazaki 444-8585, Japan

E-mail: yskwon@skku.ac.kr

Received 20 August 2004, in final form 30 September 2004
Published 5 November 2004
Online at stacks.iop.org/JPhysCM/16/8323
doi:10.1088/0953-8984/16/46/018

Abstract

We report on the magnetic susceptibility, specific heat and electrical resistivity of the heavy fermion compounds $CeNiGe_{2-x}Si_x$ ($0 \leqslant x \leqslant 1$). Compounds with $x < 1$ show antiferromagnetic order, which with increasing x shifts toward lower temperature owing to increased exchange coupling between the localized 4f magnetic moments and conduction electrons. Eventually, the magnetic order almost becomes absent, for $x = 1$. An anomaly observed in the specific heat is well interpreted by the Kondo model for a degenerate impurity spin $J = 1/2$ in the Coqblin–Schrieffer limit. A coherence peak indicative of the formation of a Kondo lattice is found in the electrical resistivity, whose features are consistent with the results for the specific heat. Interestingly, there is a significant deviation from Fermi-liquid behaviour at the critical concentration $x = 1$. This deviation is attributed to a quantum phase transition in a model with two-dimensional antiferromagnetic fluctuations.

[7] Author to whom any correspondence should be addressed.

1. Introduction

Ce-based ternary intermetallic compounds exhibit a wide range of physical properties such as long-range magnetic ordering, the Kondo effect, heavy fermion behaviour, and valence fluctuations, which arise from competition between Kondo and Ruderman–Kittel–Kasuya–Yosida (RKKY) interactions [1, 2]. The formation of a local Kondo singlet depends exponentially on the exchange interaction J: $T_K \propto 1/\exp(-1/N_F J)$, while the formation of long-range order of localized magnetic moments depends quadratically on J: $T_{RKKY} \propto (N_F J)^2$ [2, 3], where $N_F J$ is a dimensionless effective exchange coupling constant for coupling between 4f localized magnetic moments and conduction electrons with the density of states N_F at the Fermi level. For small values of $N_F J$, a local-moment magnetism (LMM) is dominant, while for larger values of $N_F J$, the valence fluctuation (VF) behaviour becomes stronger. Just at the borderline between the LMM regime and the VF regime, the heavy fermion (HF) behaviour is anticipated.

Non-Fermi-liquid (NFL) phenomena have recently been observed in the region of the transition from magnetic order to a nonmagnetic ground state; this has been one of the most interesting subjects in condensed matter physics. The experimental characteristics of NFL behaviour are power-law temperature dependences of the electrical resistivity, $\rho \propto T^n$ with $n < 2$, and the magnetic susceptibility, $\chi \propto T^{-n}$ with $n < 1$. The specific heat divided by temperature follows a logarithmic temperature dependence, $C/T \propto -\ln T$. Theoretical scenarios put forward for the NFL phenomena include

(i) a multichannel Kondo impurity model in which several channels of noninteracting conduction electrons are antiferromagnetically coupled to the Kondo-like impurity spin [4, 5],
(ii) a disorder induced distribution of the Kondo temperature of local moments [6, 7],
(iii) a second-order quantum phase transition to a magnetic state at the zero-temperature limit that is a quantum critical point (QCP) [8–10], and
(iv) a Griffiths phase which is characterized by magnetic clusters in a nonmagnetic background [11, 12].

The aim of this work is to change the exchange coupling via chemical substitution and to change the ground state continuously from the LMM regime to the VF limit, paying special attention to the critical concentration where the magnetism is completely suppressed. For this investigation we chose the ternary compounds $CeNiGe_{2-x}Si_x$. $CeNiGe_2$ shows a strong anisotropic local-moment magnetism with two-step antiferromagnetic phase transitions at $T_N^I = 3.7$ K and $T_N^{II} = 2.9$ K and a heavy fermion behaviour with a large Sommerfeld coefficient $\gamma = 97.6$ mJ mol^{-1} K^{-2} [13], whereas $CeNiSi_2$ is a valence fluctuation system with rather large $\gamma = 57$ mJ mol^{-1} K^{-2} [14]. Thus, it could be of interest to know how the exchange coupling changes on substituting silicon for germanium and how the Doniach-type phase diagram in this heavy fermion system is constructed. Although preliminary results on the magnetic susceptibility and resistivity were previously reported [15], in this paper we present a comprehensive report together with a theoretical analysis of the overall physical properties of $CeNiGe_{2-x}Si_x$.

2. Experiment

The single crystals of $CeNiGe_{2-x}Si_x$ ($0 \leqslant x \leqslant 1$) were grown by the Czochralski pulling method using a tetra-arc furnace in an argon atmosphere and then annealed at 900 °C for three weeks in an evacuated quartz tube. We used starting materials of high purity: cerium (99.9 at.% pure), nickel (99.95 at.% pure), and germanium and silicon (99.999 at.% pure). Our single

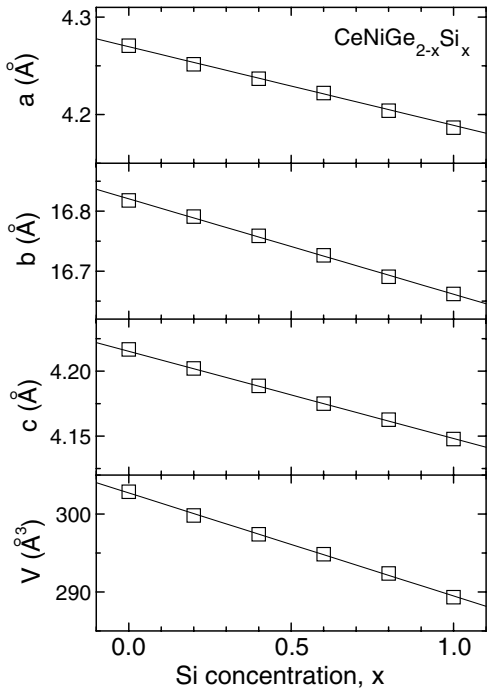

Figure 1. Lattice constants a, b, and c and unit volume V versus Si concentration x for $CeNiGe_{2-x}Si_x$ compounds.

crystal, confirmed by an x-ray Laue diffraction method, has a cylinder shape with diameter 7 mm and length 200 mm and has no cleavage. In [13], however, the single crystal of $CeNiGe_2$ grown by a Sn-flux method has a small layered shape with a shorter length along the b axis, although it is found to have the same crystalline structure as our crystal. This difference of crystal shape seems to cause the anisotropy of the physical properties of the single crystal reported on in [13] to be larger than that of our single crystal.

Powder x-ray diffraction patterns revealed crystallization in the orthorhombic $CeNiSi_2$-type (space group $Cmcm$) structure. The lattice constants a, b, and c have been determined from the positions of the Bragg reflections of the powder pattern. Figure 1 shows the Si concentration (x) dependence of the lattice constants and of the unit volume. The lattice constants and the unit volume decrease linearly with increasing x, i.e. obeying a Vegard law.

The magnetic susceptibility was measured using a Quantum Design superconducting quantum interference device (SQUID) magnetometer from 2 to 300 K at $H = 1$ kG. The specific heat was investigated by an adiabatic method with a home-made conventional ^{3}He apparatus. The electrical resistivity was measured by the conventional dc four-probe method from 0.5 to 300 K using the same ^{3}He apparatus. Since the anisotropic properties in the ac plane are negligible, we have studied the anisotropic properties with current and magnetic field along the b axis ($\|b$) and in the ac plane ($\perp b$).

3. Results

3.1. Magnetic susceptibility

Figures 2 and 3 show the inverse magnetic susceptibility $1/\chi(T)$ of $CeNiGe_{2-x}Si_x$ in a field of 1 kG for $H \perp b$ and $H \parallel b$ as a function of temperature from 2 to 300 K.

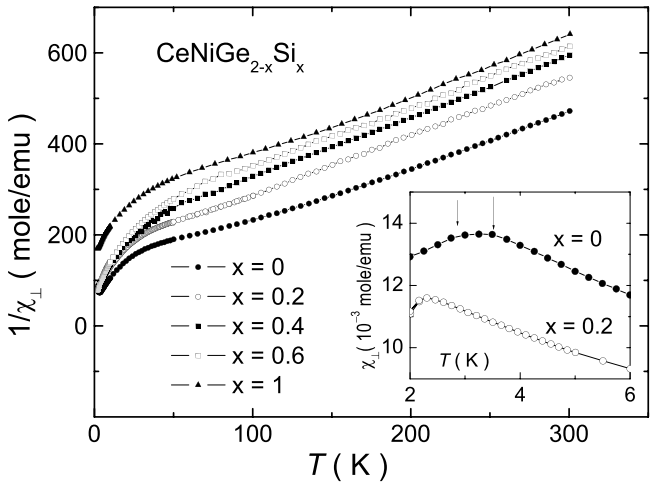

Figure 2. The temperature dependence of the inverse magnetic susceptibility $1/\chi(T)$ for $H_{\perp b}$ in $CeNiGe_{2-x}Si_x$. The inset shows an enlarged picture of the low temperature data.

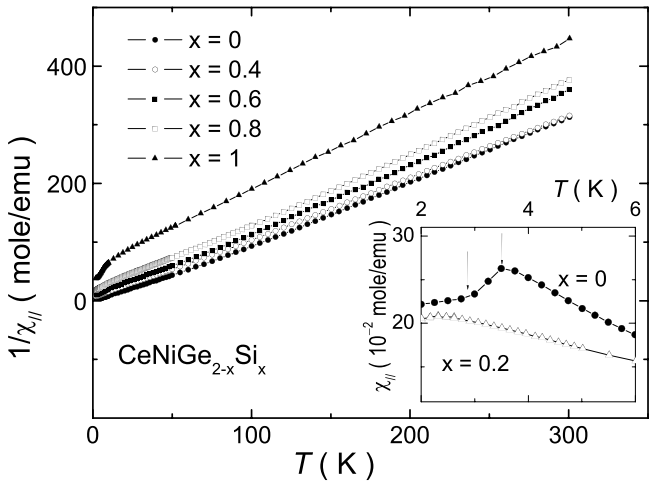

Figure 3. The temperature dependence of the inverse magnetic susceptibility $1/\chi(T)$ for $H \parallel b$ in $CeNiGe_{2-x}Si_x$. The inset shows an enlarged picture of the low temperature data.

The in-plane magnetic susceptibility $\chi_{\perp b}$ is much smaller than the b axis magnetic susceptibility $\chi_{\parallel b}$ over the measurement temperature region. Above 150 K, the data obey the Curie–Weiss law $\chi = \chi_0 + C/(T - \theta_P)$, where χ_0 is composed of the temperature-independent Van Vleck, conduction electron paramagnetic, and core electron diamagnetic contributions. In this fitting, χ_0 was varied from 0.8×10^{-4} to 2.0×10^{-4} emu mol^{-1}, which is negligibly small compared with the measured value of the overall $\chi(T)$. All compounds reveal an effective paramagnetic moment of $\mu_{\text{eff}} \approx 2.56\ \mu_B$, close to the value of the full Ce^{3+} moment (2.54 μ_B). The estimated paramagnetic Curie temperatures $\theta_{\parallel b}$ ($\theta_{\perp b}$) for $H \parallel b$ ($H \perp b$) are changed from +29 to −55 K (from −92 to −185 K) with increasing Si concentration x, as shown in figure 4. The anisotropy of θ_P is presumably due to the effect of the crystalline electric field (CEF). This might also indicate the development of an antiferromagnetic exchange interaction and/or the

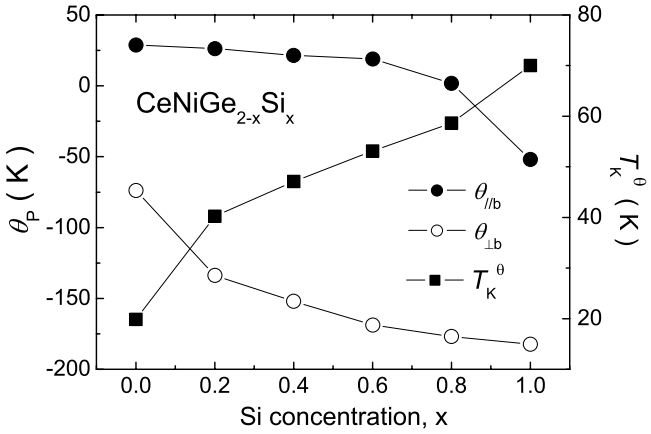

Figure 4. The paramagnetic Curie temperature θ_P for $H_{\perp b}$ and $H_{\parallel b}$ and the Kondo temperature T_K^{θ} estimated from the θ_P value versus the Si concentration x for $CeNiGe_{2-x}Si_x$.

enhancement of the Kondo interaction, which is expected to increase with x. We will discuss this point in more detail in a later part of the paper. From the value of $\theta_P = (\theta_{\parallel b} + 2\theta_{\perp b})/3$, we can roughly calculate the Kondo temperature $T_K^{\theta} \sim |\theta_P/2|$, which increases with x from 25 to 70 K as seen in figure 4. The deviation from the Curie–Weiss behaviour below 150 K could be attributed to the CEF effect. As shown in the insets of figures 2 and 3, the low temperature data for $\chi_{\parallel b}$ and those for $\chi_{\perp b}$ at $x = 0$ exhibit two anomalies, at $T_N^{I} = 3.7$ K and $T_N^{II} = 2.9$ K, indicating antiferromagnetic ordering; these are similar to the data reported by Jung *et al* [13]. They proposed anisotropic magnetic phases where the magnetic moments are strongly aligned along the b axis antiferromagnetically, while the moments in the ac plane form an incommensurate or canted noncollinear spin structure in the antiferromagnetic ordering. The two magnetic transitions are reduced to one with increasing x; $T_N = 2.3$ K at $x = 0.2$, and then no anomaly for $x > 0.2$ is observed at temperatures down to 2 K in our susceptibility measurements.

3.2. Specific heat

The 4f electron contribution to the specific heat, given by $C_{4f} = C(CeNiGe_{2-x}Si_x) - C(LaNiGe_{2-x}Si_x)$, of $CeNiGe_{2-x}Si_x$ is depicted in figure 5. For $x = 0$, two peaks are found at T_N^{I} and T_N^{II}, which correspond to the antiferromagnetic transitions observed in $\chi(T)$. The two magnetic transitions become one transition with increasing x. At $x = 0.2$, there is only one peak at $T_N = 2.3$ K, and with further increase of x up to 0.8, the peak is suppressed and shifts toward lower temperatures. Eventually, the transition becomes absent at the critical concentration $x = 1$. Above 15 K, the increase of C_{4f} with temperature could be attributed to the Schottky anomaly of the CEF. In the orthorhombic symmetry, the $J = 5/2$ degenerate states of the Ce^{3+} ion split into three doublets. Since the specific heat for the CEF structure has a peak at a temperature equivalent to about 2/5 times the energy difference between the doublets, one can understand that the energy difference for our system is larger than 80 K. In addition, there is a shoulder around 8 K for all the compounds, even though it is not distinct for the others except for $x = 1$. The C_{4f} value at 8 K for $x = 1$ is about 1.5 J mol^{-1} K^{-1}, which is of nearly the same magnitude as expected from the Coqblin–Schrieffer (CS) model for $J = 1/2$ with $T_0 = 13.5$ K ($T_K = 17$ K) as shown in the inset of figure 5 [16, 17]. Deviations

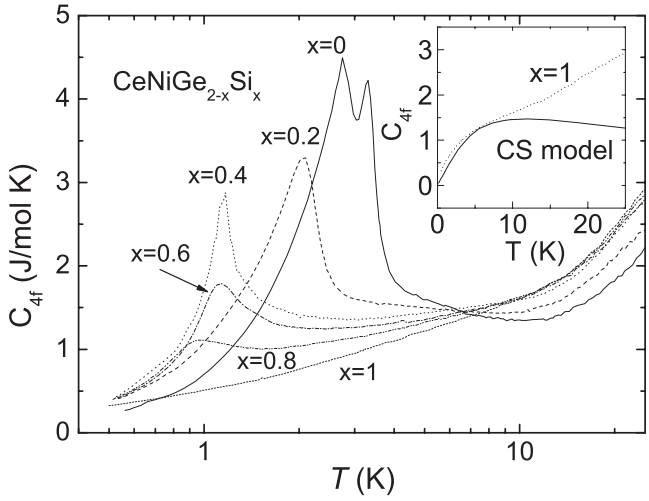

Figure 5. The temperature dependence of the 4f electron contribution to the specific heat C_{4f} in $CeNiGe_{2-x}Si_x$. The inset shows C_{4f} for $x = 1$ and the specific heat calculated from the Coqblin–Schrieffer model for $J = 1/2$ with $T_0 = 13.5$ K.

Table 1. The electronic contribution to the specific heat γ, the Kondo temperature T_K^{γ} calculated from the γ value, and the Kondo temperature T_K estimated from the Coqblin–Schrieffer model with the Si concentration x of $CeNiGe_{2-x}Si_x$.

x	γ (mJ mol^{-1} K^{-2})	T_K^{γ} (K)	T_K (K)
0	430	13.1	5.2
0.2	667	8.4	7.7
0.4	570	9.8	12.9
0.6	532	10.6	14.2
0.8	522	10.8	15.5
1	—	—	17.4

between them are observed in low and high temperatures regions. The former is ascribed to the NFL effect, which will be mentioned later, and the latter is due to the CEF effect.

In general, the specific heat due to the CEF effect in Kondo compounds is changed by the Kondo effect of the ground state. According to the degenerate Kondo model, in the presence of a CEF [18], however, the specific heat caused by the CEF effect remains almost unchanged when $A/T_K > 4$, where A is the crystal field splitting energy. Since our system, even at the limit of $x = 1$ where T_K is expected to be the largest, satisfies the above relation, the specific heat due to the CEF for $x < 1$ is thought to be of the same magnitude as that for $x = 1$. In figure 6, we have plotted the specific heat data excluding the CEF contribution, which is obtained from the deviation in the high temperature region on applying the CS model for $x = 1$ mentioned above, versus the normalized temperature T/T_0, where T_0 is the best fitting parameter from the CS model with $J = 1/2$, in addition to the best fit of the CS model. From this fit, we were also able to obtain the Kondo temperatures T_K, which are listed in table 1. It is found that T_K increases from 5.2 K for $x = 0$–17.4 K for $x = 1$, which is consistent with the increasing trends of T_K^{θ} obtained from the magnetic susceptibility. The deviation from the fit in the high temperature region might be attributed to the uncertainty of the CEF effect mentioned

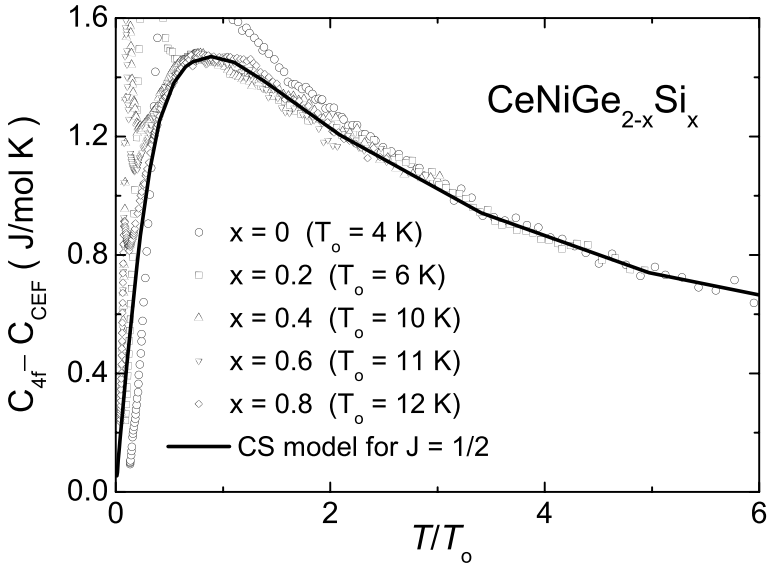

Figure 6. Scaling of the specific heat excluding the CEF effect ($C_{4f} - C_{CEF}$) versus the normalized temperature (T/T_0) for $CeNiGe_{2-x}Si_x$. The curve indicates the best fit of the specific heat calculated from the Coqblin–Schrieffer model with $J = 1/2$.

above. For $x < 1$, the predominant deviation at low temperatures is affected by the magnetic order, and for $x = 1$, the low temperature deviation is ascribed to the NFL behaviour which will be mentioned below.

Since C/T is almost linear in T^2 below $T = 0.8$ K except for $x = 1$, the electronic contribution to the specific heat is calculated by extrapolation toward the zero-temperature limit. As summarized in table 1, the Sommerfeld coefficient γ tends to decrease with increasing x except for $x = 1$. Using these values, we have determined the Kondo temperature T_K^{γ}, which is also listed in table 1, in good agreement with T_K obtained from the fits of the CS model. The decrease of γ is due to the enhancement of the Kondo interaction with x. It is particularly interesting to note that for $x = 1$ the γ value is logarithmically divergent at $T \to 0$ K with the relationship $C/T \sim \log(T_a/T)$, where $T_a = 18$ K is used, as shown in the upper panel of figure 7. This behaviour is not explained by the Fermi-liquid theory and is characteristic of non-Fermi-liquid behaviour.

The magnetic entropy S_{4f} calculated by integrating C_{4f}/T with respect to T is plotted in figure 8. It is found that S_{4f} at T_N is sufficiently smaller than $R \ln 2$ with twofold degeneracy of the CEF ground doublet, which is a sign of the substantial Kondo-derived reduction of the Ce moments. The temperature approaching the $R \ln 2$ value moves from 15 K for $x = 0$ to above 25 K for $x = 1$. This indicates that the magnetic moment reduced by the Kondo effect is gradually released towards high temperature with increasing x, again consistent with our conclusion that the Kondo temperature increases with x.

3.3. Electrical resistivity

Figure 9 shows the electrical resistivity $\rho(T)$ with the current parallel ($I \parallel b$) and perpendicular ($I \perp b$) to the b axis after normalization to the room temperature value. The in-plane resistivity $\rho_{\perp b}$ is smaller than the b axis resistivity $\rho_{\parallel b}$. For all the compounds, a broad maximum is

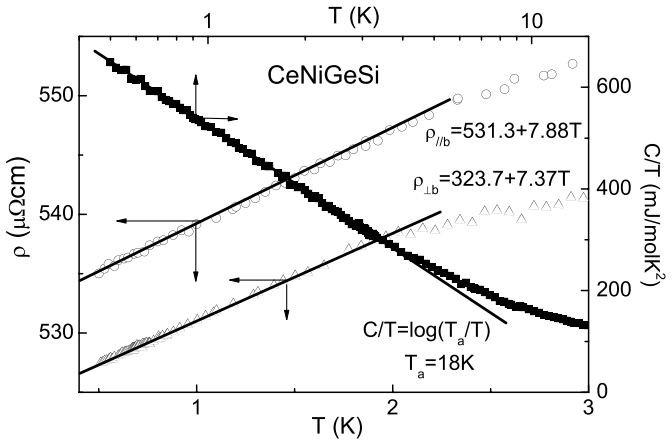

Figure 7. Specific heat divided by temperature C/T as a function of the logarithmic scale of temperature and the temperature dependence of the electrical resistivity $\rho(T)$ for $I \parallel b$ and $I \perp b$ in CeNiSiGe. For clarity, the resistivity for $I \perp b$ is shifted in the positive direction by 200 $\mu\Omega$ cm.

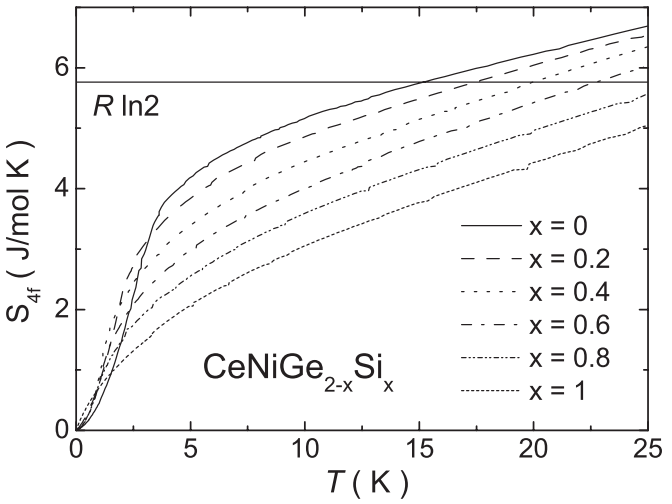

Figure 8. The temperature dependence of the magnetic entropy S_{4f} for $CeNiGe_{2-x}Si_x$.

observed at about 100 K. The magnetic contribution to the resistivity of $CeNiGe_2$ obtained by subtracting the resistivity of $LaNiGe_2$ exhibits ln T behaviour above 100 K, which is not shown here. Such behaviour could be attributed to the Kondo effect, considering the CEF effect. For $x \leqslant 0.4$, one can find a single-ion Kondo minimum, which is followed by a steep decrease due to the magnetic ordering and the onset of the coherence effect of the Kondo lattice. With increasing x, the temperature of the Kondo minimum moves almost linearly from 22 K for $x = 0$ to 26 K for $x = 0.4$, indicating increase of the Kondo interaction. The low temperature maximum located just above the antiferromagnetic transition temperature decreases from 4 K for $x = 0$ to 2 K for $x = 0.6$. For $x = 1$, the interesting point is that $\rho_{\|b}$ and $\rho_{\perp b}$ are linear with temperature over a relatively wide range from 0.5 to 2.2 K, as seen in the lower panel of figure 7, with the relationships $\rho_{\|b} = 531.3 + 7.88$ T and $\rho_{\perp b} = 323.7 + 7.37$ T ($\mu\Omega$ cm).

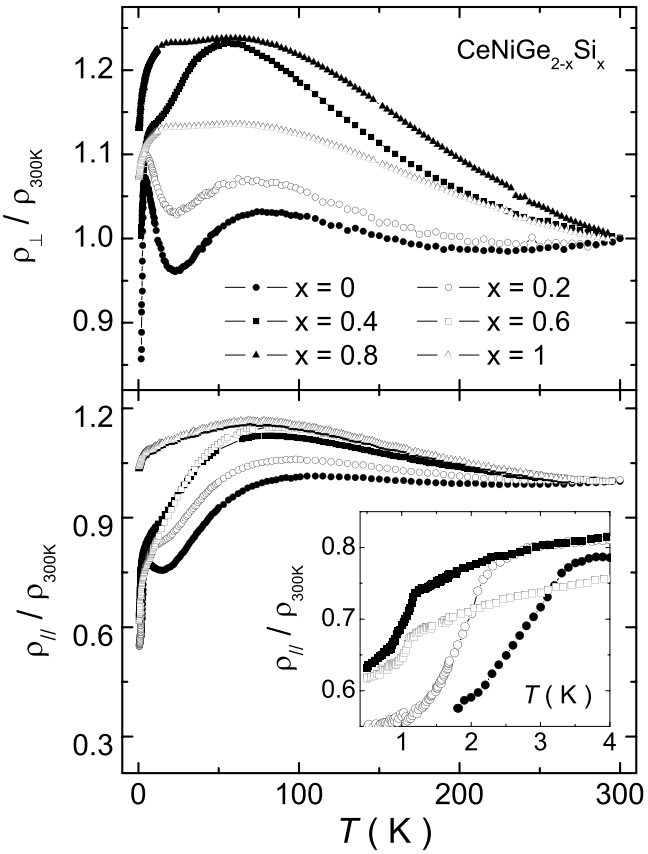

Figure 9. The temperature dependence of the electrical resistivity $\rho(T)$ for $I \perp b$ (upper panel) and $I \parallel b$ (lower panel) in $CeNiGe_{2-x}Si_x$. The inset shows the low temperature behaviour.

This behaviour could be explained by a non-Fermi-liquid phenomenon, consistent with the results for the specific heat (see figure 7).

4. Discussion

4.1. The Doniach-type phase diagram

Using the results on the magnetic susceptibility, specific heat, and electrical resistivity we can construct a Doniach-type phase diagram for the series of $CeNiGe_{2-x}Si_x$. Two characteristic temperatures, T_K and T_N, as a function of the Si concentration x, are plotted in figure 10. The Kondo temperature T_K was estimated from the application of the Coqblin–Schrieffer model with $J = 1/2$ to the measured specific heat. The antiferromagnetic transition temperature T_N was determined from the inflection point lying just above the peak temperature in the specific heat. The results demonstrate that the increase of the Kondo interaction is accompanied by suppression of the magnetic order. With $T_K \sim \exp(-1/N_F J)$, $\ln T_K$ should be inversely linear in $N_F J$. The inset of figure 10 shows the x dependence of $1/\ln T_K$, which is linear in x, but its slope changes at $x = 0.4$. In other words, $N_F J$ increases linearly with x but the rate of increase of $N_F J$ is slower for $0.4 \leqslant x \leqslant 1$. This result may be due to nonlinear variation of J with

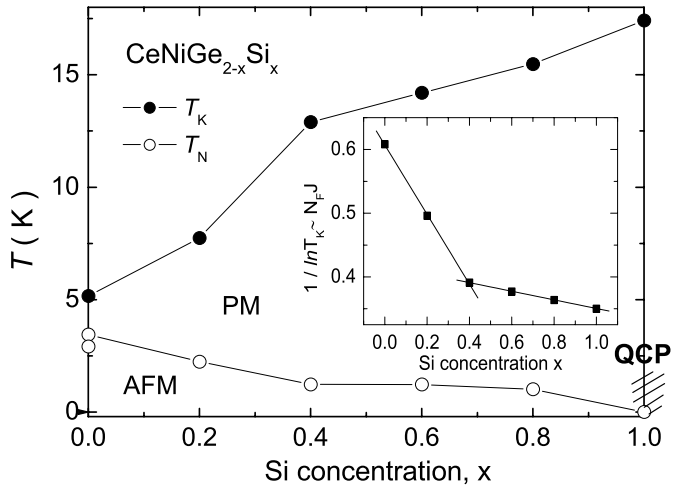

Figure 10. Two characteristic temperatures (the Kondo temperature T_K and the antiferromagnetic transition temperature T_N) versus the Si concentration x for $CeNiGe_{2-x}Si_x$. The inset indicates the x dependence of the inverse ln T_K.

varying Si concentration. The usual form of J is expressed by $J \sim V_{sf}^2/(E_F - E_{4f})$ [19], where V_{sf} is the strength of hybridization between the conduction and 4_f electrons, E_F is the Fermi energy, and E_{4f} is the energy of the 4f state. Thus, there are two possible ways to understand the origin of the increase of J with x. First, we consider the contraction of the lattice constants as we go from $x = 0$ to 1. Such a contraction gives rise to an increase of the wavefunction overlap between the conduction and 4f electrons, so the strong hybridization V_{sf} could lead to the increase of J. Secondly, we note the difference between the energy of the Fermi level E_F and that of the 4f state E_{4f}. As reported previously from photoemission experiments [20], the 4f level moves closer to the Fermi level with increasing x, making J bigger.

4.2. Non-Fermi-liquid behaviour

Another important part of this work is the observation of NFL phenomena close to the borderline, i.e. $x = 1$, from magnetic order to the nonmagnetic heavy electron ground state. For a three-dimensional system with antiferromagnetic interactions [8, 9] we expect the following temperature dependence: $\rho(T) = \rho_0 + A'T^{3/2}$, $C/T = \gamma_0 - \alpha\sqrt{T}$, and $\chi \propto T^{3/2}$. On the other hand, for a two-dimensional system with antiferromagnetic interactions [8, 9], a slightly different temperature dependence is expected: $\rho(T) = \rho_0 + A'T$, $C/T = c\log(T_0/T)$, and $\chi = \chi_0 - aT$.

As represented in figure 7, we have observed the logarithmic temperature dependence of the specific heat, $C/T \propto \ln(T_a/T)$, and the power-law temperature dependence of the electrical resistivity, $\rho = \rho_0 + AT$ at the critical concentration $x = 1$. Thus we can state that the NFL behaviours of the resistivity and specific heat observed in the same temperature region agree well with the theoretical results based on the proximity to a quantum phase transition with two-dimensional antiferromagnetic interactions. On the other hand, theoretical results based on the proximity to a quantum phase transition with three-dimensional antiferromagnetic interactions show a crossover to $\rho \propto T$ and $C/T = \gamma_0' \log(T_0'/T)$ at somewhat higher temperature [8, 9]. The crossover has been reported in the specific heat of $CeNi_2Ge_2$: $C/T = \gamma_0' \log(T_0'/T)$ seen over the temperature range of 1 K $< T <$ 3 K, while $C/T = \gamma_0 - \alpha\sqrt{T}$ is observed

for the temperature range of 0.4 K $< T <$ 1 K [21]. The resistivity of $CeNi_2Ge_2$ shows a behaviour with the exponent $n \approx 1.5$ down to 0.02 K without any sign of crossover. If the NFL behaviour of our system is due to the three-dimensional magnetic interaction, the crossover has to occur in the resistivity and specific heat below 0.5 K simultaneously. The crossover has been observed in neither of them, for our samples. On the other hand, the presence of two-dimensional magnetic interaction in $CeNiGe_{2-x}Si_x$ can be supported by their strongly anisotropic magnetism.

However, we cannot exclude with certainty the possibility that the non-Fermi-liquid behaviour observed for $x = 1$ is not due to disorder effects. For example, cubic $CeIn_{3-x}Sn_x$ has a linear resistivity at the critical value of x when $T_N > 0$ [22]. The residual resistivity of this system is two orders of magnitude higher than that of $CeIn_3$ and the disorder effect may not be neglected in the system. $UCu_{1-x}Pd_x$ is another example with clear effects due to disorder, as shown clearly from NMR and μSR measurements [23], and its NFL behaviour was subsequently analysed using a distribution of Kondo temperatures. In the Kondo disorder model, the temperature dependence of the resistivity is expected to be linear, while the specific heat coefficient C/T follows logarithmic behaviour. The residual resistivity of our sample at the critical concentration is one order of magnitude higher than that of $CeNiGe_2$ and thus we cannot disregard the effect of disorder. However, we note that the quantum critical point of our system arises precisely at the stoichiometric concentration of Ge and Si. This indicates that the disorder may not be a dominant mechanism for the NFL behaviour in our system.

Acknowledgments

This work was supported by the Korea Science and Engineering Foundation through the Centre for Strongly Correlated Materials Research (CSCMR) at Seoul National University and by grant No R01-2003-000-10095-0 from the Basic Research Programme of the Korea Science and Engineering Foundation.

References

[1] Stewart G R 1984 *Rev. Mod. Phys.* **56** 755
[2] Grewe N and Steglich F 1991 *Handbook on the Physics and Chemistry of Rare Earth* vol 14 (Amsterdam: Elsevier)
[3] Doniach S 1977 *Physica* B & C **91** 231
[4] Cox D L 1987 *Phys. Rev. Lett.* **59** 1240
Cox D L and Jarrel M 1996 *J. Phys.: Condens. Matter* **8** 9825
[5] Schlottmann P and Sacramento P D 1993 *Adv. Phys.* **42** 641
[6] Bernal O O, MacLaughlin D E, Lukefahr H G and Andraka B 1995 *Phys. Rev. Lett.* **75** 2023
Bernal O O, MacLaughlin D E, Amato A, Feyerherm R, Gygax F N, Schenck A, Heffner R H, Le L P, Nieuwenhuys G J, Andraka B, von Löhneysen H, Stockert O and Ott H R 1996 *Phys. Rev.* B **54** 13000
[7] Miranda E, Dobrosavljevic V and Kotliar G 1996 *J. Phys.: Condens. Matter* **8** 9871
Miranda E, Dobrosavljevic V and Kotliar G 1997 *Phys. Rev. Lett.* **78** 290
[8] Millis A J 1993 *Phys. Rev.* B **48** 7183
[9] Moriya T and Takimoto T 1995 *J. Phys. Soc. Japan* **64** 960
[10] Lonzarich G G 1997 *Electron* ed M Springford (Cambridge: Cambridge University Press)
[11] Castro Neto A H, Castilla G and Jones B A 1998 *Phys. Rev. Lett.* **81** 3531
[12] Griffiths R B 1969 *Phys. Rev. Lett.* **23** 17
[13] Jung M H, Harrison N, Lacerda A H, Nakotte H, Pagliuso P G, Sarrao J L and Thompson J D 2002 *Phys. Rev.* B **66** 54420
[14] Pecharsky V K and Gschneidner K A Jr 1991 *Phys. Rev.* B **43** 8238
[15] Hong S O, Mun E D and Kwon Y S 2003 *Physica* B **329–333** 514
[16] Coqblin B and Schrieffer J R 1969 *Phys. Rev.* **185** 847

[17] Rajan V T 1983 *Phys. Rev. Lett.* **51** 308
[18] Desgranges H U and Rasul J W 1987 *Phys. Rev.* B **36** 328
[19] Schrieffer J R and Wolff P A 1966 *Phys. Rev.* **149** 491
[20] Kumigashira H, Chainani A, Yokoya T, Akaki O, Takahashi T, Ito M, Kasaya M and Sakai O 1996 *Phys. Rev.* B **53** 2565
[21] Steglich F, Buschinger B, Gegenwart P, Lohmann M, Helfrich R, Langhammer C, Hellmann P, Donnevert L, Thomas S, Link A, Geibel C, Lang M, Sparn G and Assmus W 1996 *J. Phys.: Condens. Matter* **8** 9909
[22] Pedrazzini P, Gómez Berisso M, Caroca-Canales N, Deppe M, Geibel C and Sereni J G 2002 *Physica* B **312/313** 406
[23] Bernal O O, MacLaughlin D E, Lukefahr H G and Andraka B 1995 *Phys. Rev. Lett.* **75** 75
Bernal O O, MacLaughlin D E, Amato A, Feyerherm R, Gygax F N, Schenck A, Heffner R H, Le L P, Niewenhuys G J, Andraka B, von Löhneysen H, Stockert O and Ott H R 1996 *Phys. Rev.* B **54** 13000